

Frequency-dependent electrical response of holes in poly(*p*-phenylene vinylene)

H. C. F. Martens and H. B. Brom

Kamerlingh Onnes Laboratory, Leiden University, P.O. Box 9504, 2300 RA Leiden, The Netherlands

P. W. M. Blom

Philips Research Laboratories, Prof. Holstlaan 4, 5656 AA Eindhoven, The Netherlands

(Received 13 January 1999; revised manuscript received 30 June 1999)

Transport of holes in poly(*p*-phenylene vinylene) has been studied as a function of frequency, temperature, dc bias, and polymer thickness. For such a low mobility material we demonstrate that the specific frequency dependence of the response reflects the wide distribution in transit times of the injected carriers due to dispersive transport. The dc mobility is shown to correspond to the average of this dispersion and follows the empirical $\ln(\mu_{dc}) \propto \sqrt{E}$ law. [S0163-1829(99)51736-0]

The discovery of electroluminescence in poly(*p*-phenylene vinylene) (PPV) has triggered present interest in the optical and electronic properties of this conjugated polymer. The combination of easy processing and mechanical flexibility makes this material a suitable candidate for large-area applications, based on polymer light-emitting diodes (PLED's).^{1,2} One of the key parameters governing PLED performance is transport of charge carriers.

Recent dc electrical studies have pointed out that charge transport in PPV-based LED's is bulk space-charge limited.³ Current-density-voltage characterization of PPV devices under high bias conditions revealed that the dc hole mobility μ_{dc} is described by⁴

$$\mu_{dc} = \mu_0 \exp \left[-\frac{\Delta}{k_B T} + B \left(\frac{1}{k_B T} - \frac{1}{k_B T_0} \right) \sqrt{E} \right]. \quad (1)$$

The canonical technique to measure charge-carrier mobilities is the time-of-flight (TOF) experiment. In the case of nondispersive transport, the transit time τ_t of the injected charge carriers is directly related to the dc mobility, $\tau_t = L^2 / (\mu_{dc} V)$. By monitoring the emissive response of PLED's ($L \sim 100$ nm) to an applied voltage pulse, Blom *et al.* have been able to determine hole transit times in PPV.⁵ The derived hole mobilities were found to be thickness dependent, indicative of dispersive transport. According to the stochastic transport model by Scher and Montrol (SM),⁶ in the case of a long-tailed distribution of waiting times between successive hops of individual charge carriers, only the fastest carriers determine the response time. The thickness dependence of the derived "mobility" stems from the slowing down of the injected carriers. For sufficiently thick samples ($L \sim 1 \mu\text{m}$) the mobility derived from TOF becomes L independent and agrees well with Eq. (1).⁷⁻⁹

Impedance spectroscopy is a powerful technique to investigate charge transport kinetics and relaxation processes involved in solid state devices.¹⁰ In the present study the complex admittance $Y = i_{ac}/V_{ac}$ of hole-only PPV devices is examined as a function of frequency $f = \omega/2\pi$, bias voltage V_{bias} , temperature T , and polymer thickness L . Previous ac studies performed on PLED's have been analyzed in terms of equivalent RC -circuit models representing bulk and contact

regions.¹¹⁻¹⁴ In these studies no frequency dependence of the constituting elements was reported.¹⁵ The bias dependence of the PLED capacitance was interpreted in terms of charge-carrier trapping¹¹ and Schottky behavior.^{12,13} Here we demonstrate that the PLED admittance exhibits a very specific frequency dependence, which is governed by the transit of injected charge carriers. The dispersive charge transport leads to a broad distribution of transit times of individual carriers, which can be obtained from the ac response. It is shown that the average of this distribution corresponds to the dc mobility [with T and E dependence in agreement with Eq. (1)], while the transit of the fastest carriers can be described within the framework of SM theory.

The polymer used to fabricate the studied devices is OC₁C₁₀-PPV,¹⁶ the chemical structure is shown in the inset of Fig. 3. The soluble OC₁C₁₀-PPV is spin coated on top of a patterned Au contact on a glass substrate. The work function of Au lies close to the valence band of the conjugated polymer and thus can serve as a hole injector while preventing electron injection. As a top electrode evaporated Au or Cu contacts are used. Impedance measurements in the range 5 Hz–13 MHz were performed with a Hewlett Packard 4192A impedance analyzer. The analyzer can superimpose a dc voltage V_{bias} up to 35 V on the ac signal. Measurements at different oscillator levels ($V_{ac} = 10$ –250 mV) showed no dependence on V_{ac} .

Figure 1 gives the room temperature ac response of a Au/PPV/Cu device at different bias voltages. The device conductance and capacitance, taken, respectively, as $G = \text{Re}(Y)$ and $C = \text{Im}(Y/\omega)$ after correction for a contact resistance ($R_c \approx 10 \Omega$), exhibit a pronounced frequency dependence, in contrast to the assumption of a RC -circuit description. The respective capacitance traces are off-set by 0.5 nF for clarity. The solid lines represent fits to a space-charge-limited current (SCLC) model for the ac response. The $V_{bias} = 0$ V ac response is characteristic for that of a disordered insulator. The slow decrease of C and strong increase of G with frequency reflect the relaxation of permanent dipoles present in the material. The disordered nature of the polymer material gives rise to a distribution of dipolar relaxation times; the dielectric response can be accurately described by the empirical Cole-Cole equation¹⁷

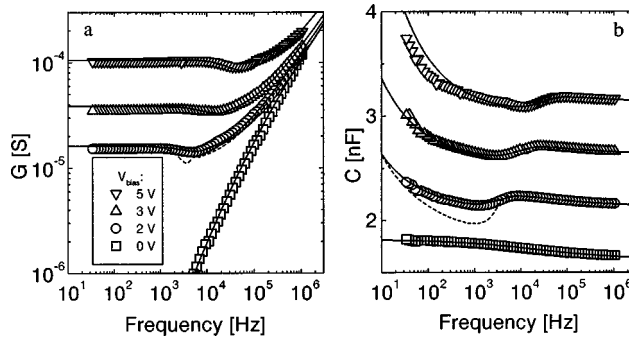


FIG. 1. (a) Frequency dependent conductance G and (b) capacitance C as function of applied bias voltage of a Au/PPV/Cu device; the respective capacitance traces are off-set by 0.5 nF for clarity. The drawn lines are fits to a SCLC model incorporating the transit time dispersion. The dashed line shows the result when this dispersion is omitted.

$$\frac{\varepsilon(\omega)}{\varepsilon_0} = \varepsilon_\infty + \frac{\varepsilon_s - \varepsilon_\infty}{1 + (i\omega\tau_0)^{1-\beta}}. \quad (2)$$

The data at 0 V shown in Fig. 1 are directly fitted to Eq. (2) giving $\varepsilon_s=2.11$, $\varepsilon_\infty=1.88$, $\tau_0=8.6$ μ s, and $\beta=0.60$. Application of a bias voltage leads to a measurable (dc) conductance and a decrease of the capacitance at low frequencies, see Fig. 1. Apparently, at low frequencies, a negative contribution to the device capacitance appears. The characteristic frequency at which this contribution disappears, shifts to higher values with increasing bias voltage. The disappearance of the negative contribution to C corresponds to a small depression of G followed by a strong increase with increasing frequency.

In a SCLC device v_{ac} probes the existing space charge in the device and injects new carriers. The time scale for the build up of additional space-charge is given by the transit time τ_t of injected carriers. At frequencies $\omega < \tau_t^{-1}$ the extra carriers lead to an additional current, which lags behind the ac stimulus. Since $Y=i_{ac}/v_{ac}$, the phase of Y decreases resulting in an apparently inductive (negative) contribution to the capacitance. At high frequencies, the period of the applied ac field is too short to redistribute the space-charge in the device. Consequently, the inductive contribution to the admittance disappears and the measured capacitance equals the geometrical value, $C=\varepsilon A/L$. Due to disorder, the transit times of individual carriers in PPV are strongly dispersed.⁵ As the finite transit time of injected carriers gives rise to an inductive contribution to the admittance, the distribution of transit times will be reflected in the frequency dependent electrical response of the device.

In order to describe the ac response of a biased PLED we resort to the basic equations for time dependent injection of space-charge-limited current:¹⁸

$$q\rho(x,t)\mu(t)E(x,t) + \varepsilon \frac{\partial E(x,t)}{\partial t} = J(t),$$

and

$$(\varepsilon/q) \frac{\partial E(x,t)}{\partial x} = \rho(x,t)$$

with $\rho(x,t)$ the time dependent local hole density and ε the dielectric constant of the polymer. The mobility μ is taken time dependent; this is a result of the dispersive transport as discussed below Eq. (4). An ideal (Ohmic) injecting contact is modeled by the boundary condition $E(0,t)=0$. In the case of a field-independent mobility the steady-state solution of the above equations is given by the famous Mott-Gurny square law, $J=9/8\varepsilon\mu_{dc}V^2/L^3$. The steady-state and time dependent contributions are separated by introducing $E(x,t)=E_{dc}(x)+e(x,t)$, $\rho(x,t)=\rho_{dc}(x)+\varrho(x,t)$ and $J(t)=J_{dc}+j(x,t)$. For small time-dependent signals the resulting equations may be linearized, giving

$$q\mu(t)\rho_{dc}e(x,t) + \varepsilon\mu(t)E_{dc}\frac{\partial e(x,t)}{\partial x} + \varepsilon\frac{\partial e(x,t)}{\partial t} = j(t). \quad (3)$$

Three contributions to $j(t)$ can be identified. The first term on the left-hand side of Eq. (3) describes the response of the “background” charge density in the device. The second term gives the current due to the additional time-dependent injected charge-carrier density, the last contribution stems from the dielectric displacement. After Fourier-transforming, the above equation can be solved analytically in the case of field-independent mobility¹⁹ and the complex admittance $Y=i_{ac}/v_{ac}$ is obtained as

$$Y(\Omega) = \frac{\varepsilon A}{\tau_t L} \frac{\Omega^3}{2i\tilde{\mu}(\Omega)[1-e^{-i\Omega/\tilde{\mu}(\Omega)}] + 2\tilde{\mu}(\Omega)\Omega - i\Omega^2}, \quad (4)$$

with the normalized frequency $\Omega=\omega\tau_t$, and normalized mobility $\tilde{\mu}(\Omega)=\mu(\Omega)/\mu_{dc}$. For $\Omega \ll 1$, we obtain $G=9\varepsilon\mu_{dc}VA/(4L^3)$ ($=\partial J/\partial V$) and $C=3\varepsilon A/(4L)$, indeed less than the geometrical capacitance $\varepsilon A/L$. Note that at low Ω the inductive contribution is independent of τ_t . At $\Omega \gg 1$, C becomes $\varepsilon A/L$.

In the sense of SM theory, dispersive transport is modeled by an algebraically decaying distribution function $\Psi(t) \propto t^{-(1+\alpha)}$ ($0 < \alpha < 1$), for the waiting time between successive hops.⁶ At short times, the average position $\langle l \rangle \propto t^\alpha$ of an injected charge-carrier packet is sublinear in time; the mobility $\mu \propto d\langle l \rangle/dt$ decreases with time. At long times, when the carriers have attained equilibrium, the drift velocity is governed by μ_{dc} . The slowing down of the carriers corresponds to a frequency-dependent mobility of the form²⁰

$$\tilde{\mu}(\Omega) = \mu(\Omega)/\mu_{dc} = 1 + M(i\Omega)^{1-\alpha}, \quad (5)$$

with M a proportionality constant. Using Eqs. (2), (4), and (5), the admittance data can be fitted, see the dashed lines in Fig. 1. Both at low and high ω the fit is in good agreement with the data, however for $\omega \sim \tau_t^{-1}$ a large discrepancy remains. Although the qualitative behavior is reproduced, the fit gives an inductive contribution to C with too sharp onset and too large value. The reason is that dispersive transport not only causes a time dependent μ , but also results in a broad distribution of transit times of individual carriers,⁶ that will “smear out” the inductive contribution around $\omega \sim \tau_t^{-1}$. The transit time distribution $P(\tau_t)$, which must be taken into account, is related to $\Psi(t)$. To our knowledge no tractable relation between these two functions is available

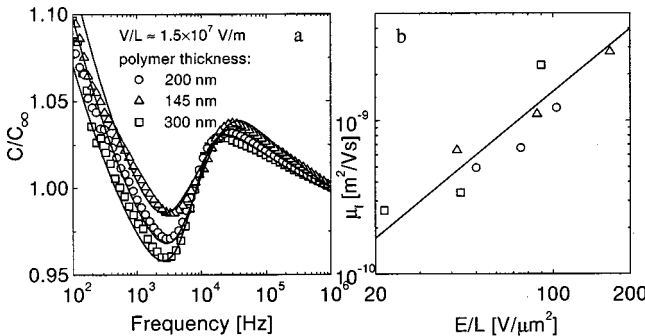


FIG. 2. (a) Normalized capacitance C/C_∞ of Au/PPV/Cu devices as a function of the polymer layer thickness fitted to the SCLC model. (b) Derived ‘mobility’ of the fastest holes, μ_f , as a function of E/L . The drawn line represents the SM scaling law $\mu_f \propto (E/L)^{(1-\alpha)/\alpha}$, with $\alpha=0.45$.

yet, which leads us to make the following simplification. The underlying mechanism of dispersive transport is the exponential dependence of the hopping probability Γ on hopping distance and hopping energy.^{6,19} As a result not only Γ , but also the mobility and transit times of the carriers will experience a broad distribution. A simple distribution function which takes this behavior into account is $P[\ln(\tau_t)] = 1/[\ln(\tau_h) - \ln(\tau_l)] \equiv 1/W$ for $\tau_l \leq \tau_t \leq \tau_h$ and $P[\ln(\tau_t)] = 0$ elsewhere. Here τ_t corresponds to the transit of the fastest carriers, while in the sense of SM theory $\tau_h \rightarrow \infty$, due to the finite probability of a carrier to encounter a transport site with an infinitely long waiting time. In reality, all injected carriers can transit the device and τ_h is finite. Since for high and low frequencies $C(\omega)$ is independent of τ_t , the dispersion in τ_t only affects the behavior in the range $\omega \sim \tau_h^{-1} - \tau_l^{-1}$. Incorporating $P[\ln(\tau_t)]$ in the analysis allows an accurate fit of the ac response of the devices.²¹ From the fitting procedure we now obtain three transport parameters, the ‘‘mobility’’ of the fastest carriers μ_f , the average mobility μ_{dc} , and the dispersion parameter α . From the fits shown in Fig. 1 $\alpha \approx 0.5$ at all V_{bias} is obtained.

Figure 2(a) displays the normalized capacitance C/C_∞ as a function of the thickness L of the polymer layer, in all cases the applied field $V/L \approx 15$ V/μm. Upon increasing L the negative contribution to C becomes more pronounced, reflecting that for thicker devices the τ_t distribution ($\sim W$) narrows. This demonstrates the relaxation of the dispersive transport towards equilibrium. For short transit times, when carriers have only made few hops, a broad distribution of charge carrier velocities exists. For long τ_t , i.e., after many hopping events, on average all carriers drift at velocity $E\mu_{dc}$. Consequently, W decreases with L . Figure 2(b) shows the derived mobility of the fastest holes versus E/L . Fitting to the SM scaling law $\mu_f \propto (E/L)^{(1-\alpha)/\alpha}$ gives an independent estimate of $\alpha=0.45 \pm 0.05$. The agreement between the α values determined from the E/L and ω response with each other and with the results of Ref. 5, support the validity of the simplified expression for $P(\tau_t)$. The average mobility derived from the data in Fig. 2(a) is 2×10^{-10} m²/Vs, independent of L . Extrapolating the L dependence of μ_f , at room temperature around $L \approx 800$ nm a crossover from dispersive to nondispersive transport is expected, as was indeed observed in Ref. 9.

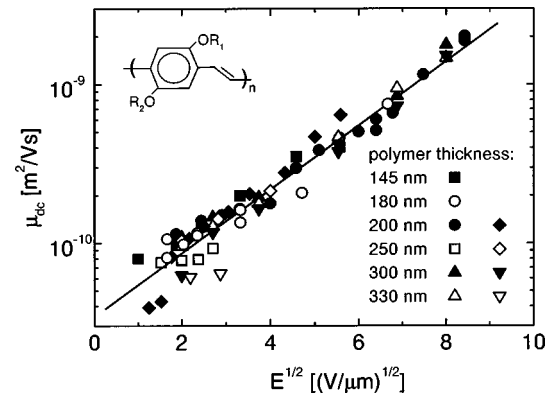


FIG. 3. Derived mobilities of several Au/PPV/Au (open symbols) and Au/PPV/Cu (closed symbols) devices with different thickness L as a function of $E^{1/2}$. The inset shows the PPV used in this study with $R_1=\text{CH}_3$ and $R_2=\text{C}_{10}\text{H}_{21}$.

In Fig. 3 the derived room temperature average mobilities of several Au/PPV/Au (180, 250, and 330 nm) and Au/PPV/Cu (145, 200, and 300 nm) devices are shown. Clearly, the obtained mobilities are independent of the material used for the cathode and L and thus represent a genuine material parameter. The independence of L proves that the dc mobility indeed corresponds to the *average* behavior of the dispersive transport.

From the T dependence of Y (not shown) it follows that with lowering T the strength of the inductive contribution to C strongly decreases, corresponding to a broadening of the transit time dispersion. Such behavior is in agreement with numerical simulations,²² and reflects the growing influence of disorder at low temperatures. The resulting hole mobilities μ_{dc} and μ_f are plotted in Fig. 4 for a device with $L=200$ nm. A simultaneous fit of the μ_{dc} data to Eq. (1) yields $\Delta=0.45$ eV, $\mu_0=8.0 \times 10^{-4}$ m²/Vs, $B=3.0 \times 10^{-5}$ eV(m/V)^{1/2}, and $T_0=500$ K, in good agreement with dc experiments.⁴ The mobility of the fastest holes is fitted to the SM scaling law

$$\mu_f \propto [l(E)/L]^{(1-\alpha)/\alpha} \exp[-\Delta_f/(k_B T)],$$

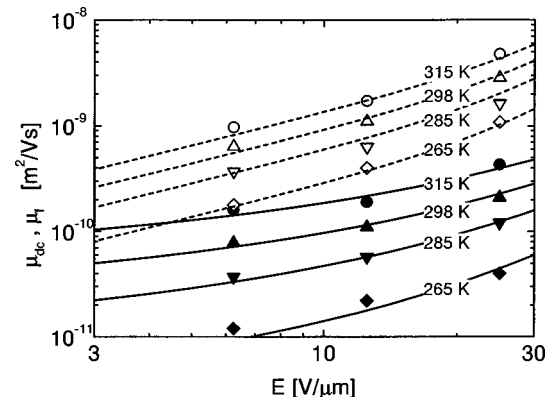


FIG. 4. Average (dc) hole mobilities (closed symbols) and mobility of the fastest holes (open symbols) as a function of electric field and temperature of a Au/PPV/Au device with $L=200$ nm. The drawn lines are a simultaneous fit of the μ_{dc} data to Eq. (1), the dashed lines represent a fit of μ_f to the SM scaling law (see text).

using the empirical expression $I(E) = \sinh[eER/(2k_B T)]^5$, with $\alpha=0.5$, $\Delta_f=0.24$ eV and $R=3$ nm. R can be interpreted as the length scale above which structural disorder appears homogeneous. Since $\Delta_f < \Delta$, the ‘‘fastest’’ carriers move along a path which circumvents the higher potential barriers, but with more structural disorder as is apparent from the stronger E dependence.

The effects of finite transit times are not only relevant for PPV-LED’s, but also for devices of other low mobility materials like most polymers, organic conductors, ionic conductors and amorphous semiconductors. To have $\tau_t^{-1} \sim \mu_{dc} V/L^2$ within the range of impedance spectroscopy

(Hz–MHz) in conventional semiconductors (where $\mu \sim 10^3$ cm²/Vs), device dimensions must be of the order of cm’s or more; in practice, common RC models suffice.

In summary, we have shown that the transit of injected carriers leads to an inductive contribution to the device admittance. From the specific frequency dependence it follows that the charge transport is characterized by the dispersion parameter $\alpha \approx 0.5$. The obtained average mobility corresponds to μ_{dc} and has the usual $\exp(\sqrt{E})$ dependence.

Valuable discussions with J.A. Reedijk, O. Hilt, and M.C.J.M. Vissenberg are gratefully acknowledged. This work was financially supported by Stichting FOM.

-
- ¹J. H. Burroughes *et al.*, Nature (London) **347**, 539 (1990).
 - ²D. Braun and A. J. Heeger, Appl. Phys. Lett. **58**, 1982 (1991).
 - ³P. W. M. Blom, M. J. M. de Jong, and J. J. M. Vleggaar, Appl. Phys. Lett. **68**, 3308 (1996).
 - ⁴P. W. M. Blom, M. J. M. de Jong, and M. G. van Munster, Phys. Rev. B **55**, R656 (1997).
 - ⁵P. W. M. Blom and M. C. J. M. Vissenberg, Phys. Rev. Lett. **80**, 3819 (1998).
 - ⁶H. Scher and E. W. Montroll, Phys. Rev. B **12**, 2455 (1975).
 - ⁷E. Lebedev *et al.*, Appl. Phys. Lett. **71**, 2686 (1997).
 - ⁸I. H. Campbell, D. L. Smith, C. J. Neef, and J. P. Ferraris, Appl. Phys. Lett. **74**, 2809 (1999).
 - ⁹M. C. J. M. Vissenberg and P. W. M. Blom, Synth. Met. **102**, 1053 (1999).
 - ¹⁰J. R. MacDonald, *Impedance Spectroscopy* (John Wiley and Sons, New York, 1987), Chap. 1, p. 2.
 - ¹¹I. H. Campbell, D. L. Smith, and J. P. Ferraris, Appl. Phys. Lett. **66**, 3030 (1995).
 - ¹²M. Esteghamatian and G. Xu, Synth. Met. **75**, 149 (1995).
 - ¹³M. Meier, S. Karg, and W. Riess, J. Appl. Phys. **82**, 1961 (1997).
 - ¹⁴Y. Li, J. Gao, G. Yu, Y. Cao, and A. J. Heeger, Chem. Phys. Lett. **287**, 83 (1998).
 - ¹⁵G. Yu *et al.*, Appl. Phys. Lett. **73**, 111 (1998), do use the f dependence of Y of PPV light-emitting electrochemical cells to distinguish electronic and ionic contributions.
 - ¹⁶C. Liedenbaum *et al.*, Synth. Met. **91**, 109 (1997).
 - ¹⁷C. J. F. Böttcher and P. Bordewijk, *Theory of Electric Polarization* (Elsevier Scientific Publishing Company, Amsterdam, 1978), Vol. II, Chap. IX, p. 62.
 - ¹⁸M. A. Lampert and P. Mark, *Current Injection in Solids* (Academic, New York, 1970), Chap. 6, p. 114.
 - ¹⁹The E dependence of μ_{dc} gives rise to a weaker than $E \propto x^{1/2}$ field distribution (Ref. 4). Since a flat distribution corresponds to an ohmic system, this suppresses space-charge effects. Numerical calculations reveal a 10–30 % less negative contribution to C . This has been taken into account in the fits of the ac response.
 - ²⁰H. Böttger and V. V. Bryksin, *Hopping Conduction in Solids* (Akademie-Verlag, Berlin, 1985), Chap. 6, p. 224.
 - ²¹A different $P[\ln(\tau_t)]$ with comparable W may also work.
 - ²²H. Bässler, Phys. Status Solidi B **175**, 15 (1993).